Running Head: Correlation of Microbial Communities with Caclium Carbonate (Travertine) Mineral Precipitation

Correlation of Microbial Communities with Calcium Carbonate (Travertine) Mineral Precipitation at Mammoth Hot Springs, Yellowstone National Park, USA

George T. Bonheyo[1, 3], Jorge Frias-Lopez[1], Héctor García Martín[2], John Veysey[2], Nigel Goldenfeld[2] and Bruce W. Fouke[1]

[1]*Department of Geology, University of Illinois at Urbana-Champaign, 1301 West Green Street, Urbana, Illinois 61801-2938, USA.*

[2]*Department of Physics, University of Illinois at Urbana-Champaign, 1110 West Green Street, Urbana, Illinois 61801-3080, USA.*

[3]*Geobiologics, University of Illinois at Urbana-Champaign, 1110 West Green Street, Urbana, Illinois 61801-3080, USA.*

Competing interests: The authors have no competing interests that might be perceived to influence the results and discussion reported in this paper.

Correspondence and request for materials should be addressed to Bruce W. Fouke (Email: fouke@uiuc.edu).

It is possible that common earth-surface geological features can arise as a result of bacteria interacting with purely physical and chemical processes. The ability to distinguish ancient and modern mineral deposits that are biologically influenced from those that are purely abiotic in origin will advance our ability to interpret microbial evolution from the ancient rock record on earth and potentially other planets. As a step toward deciphering biotic from abiotic processes, analyses of carbonate mineralogy and geochemistry have been combined with community-based microbial genetic analyses along a hot spring drainage system at Angel Terrace, Mammoth Hot Springs, Yellowstone National Park. The shape and chemistry of carbonate mineral deposits (called *travertine*) changes dramatically along the spring outflow channel, forming five distinct ecological zonations (termed sedimentary depositional *facies*). These systematic changes in travertine mineralization exhibit distinct boundaries, even though most physical and chemical attributes of the spring water change smoothly and continuously over the course of the drainage outflow path. Here, an unexpectedly sharp correlation between microbial phylogenetic diversity and travertine facies has been documented, which suggests that changes in bacterial community composition are a sensitive indicator of changing environmental conditions and associated calcium carbonate mineral precipitation along the spring outflow. These results provide an environmental context for constraining abiotic and biotic theories for the origin of distinct crystalline structures and chemistries formed during hot spring travertine precipitation.

A biocomplexity study has been initiated at Mammoth Hot Springs in Yellowstone National Park to determine whether microbial community structure and activity can influence the chemistry and morphology of calcium carbonate mineral precipitation. Carbonate minerals are ideal for this type of study because they can be precipitated at life-permitting temperatures, are sensitive to environmental conditions, and are the most ubiquitous minerals precipitated in Earth surface environments (25, 27). Subsurface waters erupt at Mammoth Hot Springs and precipitate terraced crystalline deposits, called *travertine*, which are composed of both the aragonite and calcite mineralogical polymorphs of $CaCO_3$ (2, 12). The present study was conducted at Spring AT-1, located on Angel Terrace in the Mammoth Hot Springs complex at the northern margin of Yellowstone (Fig. 1).

Hot spring water in this region has been derived from fresh rainwater and snowmelt that moved into the subsurface through fault conduits, was heated by subsurface volcanic magma chambers, chemically reacted with Mississippian-age limestones and evaporites, and returned to the surface through vents as Ca-Na-HCO_3-SO_4 type hot waters (21, 22). The drainage system of Spring AT-1 is typical of the hydrothermal features found in this area, in that as the spring water flows away from the vent it cools from 73^{o} to 25^{o} C and vigorously degasses CO_2, increases the pH from approximately 6 to 8 (10; Figs. 2 and 3). As a result, travertine is rapidly precipitated at rates as high as 5 mm/day and changes in mineralogical composition from 100% aragonite in the higher-temperature vent to nearly 100% calcite in the lower-temperature distal parts of the drainage system (10). This rapid precipitation partially to completely seals the vents and reroutes the drainage system, causing the spring flow path to regularly change in direction and intensity, which in turn influences subsequent travertine precipitation. The dynamical interplay between fluid flow and travertine precipitation, be it primarily biotic or abiotic in origin, is complex and not yet understood.

In order to evaluate the relative influence of the different physical, chemical, and biological aspects of this rapidly changing hydrothermal system, the Spring AT-1 drainage outflow was first subdivided into a series of recognizable ecological partitions along the flow path. These sub-environments, called sedimentary depositional *facies*, are based on changes in the shape and composition of the travertine that is precipitated on the floor of the spring outflow channel (10; Fig. 3). The general facies concept, first introduced nearly 170 years ago (13), holistically links specific rock and mineral types with the sum physical, chemical, and biological attributes of the environment in which the rocks and minerals were deposited (19, 31). Facies models have universal application to settings that range from lakes to glaciers to coral reefs, and are the cornerstone for paleo-environmental interpretations of the ancient rock record (29). The facies model approach was used here to systematically break down the large complex environment of the Spring AT-1 system into smaller sub-environments along the drainage outflow. Each facies is characterized by a morphologically and chemically distinct type of travertine mineral deposit (10). The drainage system systematically self-organizes into a regular succession of facies that form along the down stream flow path, which consistently re-establish themselves when the overall drainage system of any individual vent significantly changes or migrates to another location. In addition, the travertine facies model consistently forms in carbonate hot springs from other geographic locations and different geologic ages (9, 10).

It is important to recognize that the travertine facies model is created by *in situ* carbonate crystal precipitation directly from the flowing spring water, with little to no downstream transport of sedimentary particles. This is a significantly different regime from most other environments of sedimentary deposition, where water-driven sediment transport is the dominant process (29). Thus, the Spring AT-1 travertine facies model reflects the complex biotic and abiotic interactions occurring on the substrate surface and

in the directly overlying flowing spring water. An attribute unique to this environment is the extremely high rate at of mineral precipitation, which makes all physical boundaries in the spring outflow environment, including water surface tension itself (2, 10), viable crystal nucleation substrates. Therefore, the race to escape crystal entombment has significant influence on microbial lifestyles in these springs, while microbial cell walls themselves create important nucleation substrates that strongly influence the shape and form of the travertine deposits (7, 8).

The Spring AT-1 drainage system is composed a five-component succession of travertine facies (10), which have been called the vent, apron and channel, pond, proximal-slope and distal-slope facies (Figs. 2 and 3). Each facies is defined by the size, shape, structure, elemental and isotopic chemistry, and mineralogy of the calcium carbonate crystalline travertine deposits precipitated on the bottom of the drainage outflow. Within this facies framework, the physical and chemical characteristics of the spring water (e.g. temperature, pH, elemental and isotopic chemistry) have been measured and integrated with travertine mineral precipitation via quantitative water-rock interaction modeling (10). Each travertine facies can be as much as 10s of meters in length along the spring flow path and cover 100s of square meters in area. Conversely, the boundaries between facies are relatively abrupt (generally 1 to 15 cm in length along the spring flow path) despite relatively continuous changes in water chemistry (Figs. 2 and 3). The aqueous chemistry of Spring AT-1 is dominated by CO_2 degassing and dropping temperature, as proven by Rayleigh-type fractionation calculations of spring water dissolved inorganic carbon (DIC) and its associated $\delta^{13}C$ (10). While these physical factors help drive the rapid precipitation of carbonate crystals to deposit travertine at remarkably high rates, they are not the exclusive controls on precipitation. Significant biological controls on travertine crystal form and isotope chemistry have been identified where travertine crystals entomb and preserve the shape of filamentous *Aquificales*

bacteria, and by quantitative subtraction of degassing and temperature effects on $\delta^{13}C$ and $\delta^{18}O$ isotopic fractionation in the spring water and the travertine (10). These robust disequilibrium signatures may be biologically mediated and systematically increase in magnitude from the high to the low temperature portions of the outflow.

A culture-independent molecular survey was completed of the microbial communities inhabiting Spring AT-1 within the context of the travertine facies model (11). PCR amplification and sequencing of 16S rRNA gene sequences with universally conserved bacterial primers was used to identify over 553 unique partial and 104 complete gene sequences, which were derived from 1050 sequences from a total pool of more than 14,000 clones using restriction fragment length polymorphism (RFLP) screening (described below). The partial and complete gene sequences are affiliated with 221 unique species that represent 21 bacterial divisions. These sequences exhibited less than 12% similarity in bacterial community composition between each of the travertine depositional facies. This implies that relatively little downstream bacterial transport and colonization take place despite the rapid and continuous flow of spring water from the vent to the distal-slope facies (Figs. 2 and 3). These results suggest that travertine depositional facies, which are independently determined by the morphology and chemistry of the travertine deposits, may effectively predict bacterial community composition (11).

The present study is a rigorous statistical evaluation of the facies-specific 16S rRNA gene sequence clone libraries collected from Spring AT-1, and represents the first such quantitative study of molecular microbiology conducted within the ecological context of a depositional facies model. This facies-based analysis will permit the results to be

directly applied to environmental interpretations of ancient travertine deposits, and could have direct applicability with respect to approach, ecological context, and techniques for many other terrestrial and marine environments of sediment deposition.

MATERIALS AND METHODS

Field work and sample collection. A total of 50 spring water and substrate samples were collected during daylight hours from the interior of each of the five travertine facies at Spring AT-1. Field photographs and detailed diagrams depicting aerial and cross-sectional views of Spring AT-1 with the sampling positions, have previously been published (10, 11). Spring water was collected in acid-cleaned 1 liter Nalgene HDPE bottles. The water was hand-pumped through a sterile 0.45 μm filter-loaded cup (Pall/Gelman). All filters were then immediately frozen at –20^{o}, transported to Illinois on dry ice and stored at -40^{o} to -80^{o} C. Substrate samples were collected by removing a 2 cm^{2} portion of the uppermost 0.25 to 1 cm of the floor of each facies with an acid-cleaned spatula. Samples were then placed in a sterile disposable 15 ml polypropylene centrifuge tube, immersed in 80% ethanol, and crushed and homogenized in sterile 15 ml polypropylene centrifuge tubes with sterile blades, creating a slurry of ethanol, microbial mats, loose microorganisms, and travertine crystals.

DNA extraction, PCR amplification, cloning and sequencing. The DNA extraction protocols and 16S rRNA gene sequence PCR amplification protocols have previously been described (11), the critical aspects of which are briefly reviewed here. Bead beating (14), freeze-thaw cycling, and chemical lysis protocols (20) were used to extract community genomic DNA from the cells collected on the filters and the substrate slurries. For both the bead beating and freeze-thaw techniques, a 400 μl aliquot of the

lysate was used for additional DNA precipitation using 2 volumes absolute ethanol, followed by a series of washing steps using 70% EtOH (20). The ethanol precipitated lysates, untreated lysates, and untreated samples were used in subsequent PCR reactions. Total environmental chromosomal DNA was used as template for PCR amplification of 16S rRNA genes using a Mastercycler Gradient thermocycler (Eppendorf, Westbury, NY) and universal bacterial 16S rRNA primers obtained from Operon Technologies, Inc. (Alemeda, CA). B. Paster (personal communication) provided the sequence of each primer: forward primer: 28F (5'-GAGTTTGATYMTGGCTC); reverse primer: 1492R (5'-GYTACCTTGTTACGACTT). Reaction mixtures included a final concentration of: 1X TaqMaster buffer (Eppendorf), 1X TaqM enhancer (Eppendorf, Westbury, NY), 0.2 mM each dNTP (Gibco/BRL, Rockville, MD), 200 ng each of forward and reverse primers, 5-30 µl of the sample preparation, and water to bring the total volume to 100 µl. After standard amplification, 8 µl of PCR product was transferred to a new well of a 96-well microtiter plate containing 32 µl of restriction digest mixture consisting of the 4-base recognition site enzymes *Msp*I and *Hin*P1 I in 1x NEB Buffer 2 (New England Biolabs, Beverly, MA). The digest products were then separated by electrophoresis on a 3.0% agarose gel (MetaPhor; BioWhittaker Molecular Applications, Rockland, ME) stained with ethidium bromide and the RFLP patterns used to identify unique clones were submitted for sequence analysis. Three to five samples with identical RFLP patterns were selected for sequence analysis in an effort to capture different sequences with similar RFLP patterns. Inoculation, cell culturing, template preparation, and sequencing were performed at the University of Illinois Urbana-Champaign W. M. Keck Center for Comparative and Functional Genomics. To generate nearly complete sequences, unique clones were selected based on the sequences generated from the T7(-26) primer (24) and the remainder of the 16S sequence was determined using either the M13(-24) or M13(-48) primer (28). Two other primer pairs within the 16S rRNA gene sequence were also used, which included: (1) Bact343Fwd. 5'-TACGGRAGGCAGCAG and Bact 1115Rev.

5'-AGGGTTGCGCTCGTTRC (30); and (2) 805aF 5'- ATTAGATACCCYGGTAGTC and 926/20 5'-CCGTCAATTYYTTTRAGTTT (14, 30). Contiguous sequences were assembled manually with the DNA analysis software Sequencher 4.1 (Gene Codes Corp., Ann Arbor, MI). Ultimately, 657 partial 16S rRNA gene sequences were obtained, and 108 of these were sequenced as contigs to completion.

Nucleotide sequence accession numbers. The GenBank accession numbers for the 16S rRNA gene sequences analyzed in this study are AF445645 through AF446346.

RESULTS

Operational Taxonomic Units: Bacterial clone 16S rRNA gene sequence libraries were constructed for the vent, apron and channel, pond, proximal-slope and distal-slope travertine facies at Spring AT-1 (11). The number of base pairs comprising each these 16S rRNA gene sequences, the species-level and division-level similarity match at 97% or greater with affiliated microoganisms in GenBank, and the occurrence or absence of each gene sequence within each travertine depositional facies, have been published (11). In the present study, gene sequences from the Spring AT-1 clone libraries were grouped into three “percent difference” cut-offs in 16S rRNA gene sequences (0.5%, 1%, and 3%) with respect to comparison with published sequences in GenBank, to define three levels of Operational Taxonomic Units (OTUs; 15). The lower 0.5% bound is based on our PCR and sequence derived error rate (1, 26), while the upper 3% difference is a typical OTU definition (23). Repetitive single-stranded sequencing and editing of the same sequences gave a predicted error rate of 0.32% and the error rate for Taq polymerase, which is 0.0001 (1, 26).

The facies-specific OTU distribution for each of the three definition levels was compared to determine whether this affected the degree of facies partitioning. Using the 3% cut off, a total of 193 OTUs were identified and these exhibited 90% partitioning between facies. The 1% cut off yielded 237 OTUs that were 91% portioned between facies, while the 0.5% cut off resulted in 331 OTUs that were 93% partitioned. Therefore, the graphical representation of the distribution of sequences amongst the five facies using a 1% OTU definition (Fig. 4) is similar in appearance to the 3% and 0.5% plots. Thus, regardless of OTU definition, the facies partitioning is extremely high. As a correlative result, the total number of 16S rRNA gene sequences that were found in more than one facies was extremely low under all OTU definitions: 19 OTUs under the 3% definition, 20 OTUs under the 1% definition, and 24 OTUs under the 0.5% definition. Of importance, two of the 16S rRNA gene sequences (*Aquificales* pBB and the β-Proteobacterium OPB 30) were found in all five facies (Fig. 4).

Accumulation Curve Analyses: To quantitatively estimate how well each facies was sampled, accumulation curves were fitted to analytical curves obtained by modeling the sampling process (Fig. 5). In these accumulation curves (defined as a graph showing the proportion of novel gene sequences found with each new sample; 16), a straight line would indicate that only a small subset of the total biodiversity has been sampled. This would indicate that 100% new OTUs are detected with each additional new sample analyzed. If a facies is well sampled and thus better characterized, the curve will begin to flatten asymptotically when the number of samples (n) is large, because OTU sequences previously not found are detected with decreasing frequency.

It was assumed that in each environmental sample collected from each facies, there is a maximum of N possible bacterial cells that could be detected, and that each of these cells would be present and detected in the sample with a probability p, regardless of the

cell's identity. The factor *p* includes the combined probability of the cell being captured and detected through the process of DNA extraction and amplification of the 16S rRNA gene sequences via PCR. Multiple methods of DNA extraction were used to eliminate cell durability biases and amplify the 16S rRNA gene via PCR (11). In addition, the resultant clone library was RFLP-screened in an attempt to sequence only unique clones within that sample, as opposed to repeatedly sequencing identical clones. In this manner the likelihood was increased that an OTU will be detected even if it is not numerically dominant in the clone library, which may be an artifact of extraction, amplification, and cloning biases rather than environmental population abundance.

Given these considerations, accumulation curves were generated for each of the three different OTU definitions (3%, 1% and 0.5%) within each facies. As an example from the pond facies is shown in Figure 6. The curve from each of the three different OTU definition collapses into the same curve (Fig. 5), giving some confidence in the robustness of the sampling procedure and the validity of the assumption of random sampling used to derive the exponential accumulation curve. In this model, all of the OTUs were assumed equally likely to appear (hence the factor $1-S/S_o$, described below). In a more realistic approach, the probability of finding each new OTU should be proportional to its abundance. However, the approximations described above fit the data well (Fig. 6) and provide a tractable expression for the accumulation curve.

The likelihood that each sequence analyzed will represent a new OTU is approximated as $(1-S/S_o)$, where S is the number of different OTUs already identified and S_o is the total number of different OTUs present in the environment. For each sequence, the probability that the number of different OTUs will increase is $p(1-S/S_o)$. This leads to an accumulation curve of the type $S=S_m\,(1-\exp(-Kt))$, where t is the maximum number of individuals that would be found if $p=1$ and K is a constant related to the sampling

procedure. This is not quite what was represented in the accumulation curves (Fig. 6), since only information about samples rather than individuals has been used, as explained above. Nonetheless, the number of samples n is simply $n=t/N$, so $S=S_m\ (1-exp(-Kn))$. The parameters K and S_m were determined from a linear fit of $log(dS/dn)$ versus $-n$. Estimates through other methods were also attempted: fits to hyperbolic accumulation (6) curves were not convincing and non-parametric methods (5, 16) yielded variances that were too large to be trustworthy.

DISCUSSION

Although different microbial species have specific growth requirements and preferred temperature and pH ranges (3, 4), the tight partitioning with respect to the travertine facies is nonetheless remarkable. First, it is surprising that very few of the upstream sequences were not also detected downstream. It was initially expected that the rapid flow of the spring water would result in downstream transport of microbial cells, and thus many sequences might also be identified downstream of their point of initial detection. Consequently, most of the analyses were performed on the first four facies extending from the vent (1). Surprisingly, the sequences detected in the water column of one facies, which are presumably most susceptible to being flushed downstream, were not typically detected downstream of their original facies (Fig. 4). Secondly, because bacterial species have a preferred range of environmental growth conditions, it was expected that many sequences would be found across facies boundaries, coinciding with gradual temperature and pH changes. Instead, the facies boundaries proved to be nearly absolute thresholds with respect to detected bacterial 16S rRNA gene sequences. Although particular gene sequences were observed over a range of conditions within each

travertine facies, OTUs were not found to traverse the facies boundaries with the rare but notable exceptions of *Aquificales* pBB and β-Proteobacterium OPB 30.

Inferred metabolic activity of the identified bacteria, derived from comparison of the Spring AT-1 gene sequences to those in GenBank, indicates that the bacterial communities found in the spring drainage system change consistently: primarily chemolithotrophic Aquificales and β-Proteobacteria in the vent facies, to a variety of photoautotrophic Cyanobacteria in the pond facies, and ultimately to heterotrophic (α-Proteobacteria, δ-Proteobacteria, and BCF in the distal-slope facies (11). Associated with this transition is an observed increase in the total number of OTUs and their associated bacterial divisions from the vent to the pond facies (Fig. 4). The number of OTUs decreases, however, with down flow progression into the proximal-slope and distal-slope facies (Fig. 4). These trends in our data can be interpreted as follows. In general, fewer OTUs and their representative bacterial divisions would be expected at the upper temperature limits of the spring where little organic matter is available for heterotrophy and the temperature is at the upper limit for photosynthesis (17). Although the pond through distal-slope facies successions have temperature profiles that would support both autotrophic and heterotrophic microbial lifestyles, a reduction is actually observed in the number of species represented in the proximal-slope and distal-slope facies. Although unproven, it is possible that such variation may result from differences in the environmental stability of each facies with regards to temperature, pH, and water flow. Ponds, for example, have the widest temperature and pH range of any facies and show greater fluctuations in flow direction and intensity (10).

To validate the interpretation that the 16S rRNA gene sequences are partitioned amongst facies, it needs to be substantiated that a reasonably high proportion of the total microbial community in each facies has been identified. Otherwise, severe under-

sampling might have prevented identification of OTUs that actually do occur in multiple facies, and thus create a similar type of facies-specific distribution. Estimates for the total number of OTUs in each facies were therefore made using an exponential fit to the accumulation curve in Figure 5. As previously stated, the accumulation curve plots the number of new OTUs found in a given number of samples, versus this number of samples, *n*. Since all of the samples are assumed to be equivalent, this is an average taken over all possible permutations of these samples. Accumulation curves are traditionally made using the number of individuals as the x-axis (15) instead of the number of samples as was done in the present study. However, the Spring AT-1 samples amalgamate large numbers of individuals. Thus information is available regarding which OTUs are present in each sample, but not the OTU identity for every individual in the sample. Therefore, the abundance of unique gene sequences in the clone libraries are not necessarily representative of the abundances in the environmental sample due to the inherent DNA extraction and PCR biases. As a result, the raw clone library data cannot be used to make accumulation curves.

Given the above reasoning, accumulation curves in this study were generated for each facies based on the three different OTU definitions of 3%, 1% and 0.5% (Fig. 6). The curves from all three OTU definitions collapse into the same curve, giving confidence in the robustness of the sampling procedure and the validity of the assumption of random sampling used to derive the exponential accumulation curve. Thus, since all of the individual microbial cells are captured with equal probability, it is reasonable to expect that the observed OTUs represent the most numerically abundant bacteria in each facies. Consequently, it can be concluded that the microbial species affiliated with these OTUs, and therefore most of the bacterial consortia, are partitioned according to the travertine facies model. This finding constrains abiotic theories for the origin of travertine

terraces, in that either their origin is biotic, or else the microbial ecology is strongly coupled to the geochemistry through mechanisms presently unknown.

ACKNOWLEDGEMENTS

This research was supported by grants from the NSF Biocomplexity in the Environment Program, NSF Geosciences Postdoctoral Research Fellowship Program, Petroleum Research Fund of the American Chemical Society Starter Grant Program, and the University of Illinois Urbana-Champaign Critical Research Initiative. Conclusions reached in this study are those of the authors and do not necessarily reflect those of the funding agencies. Permission to work in Yellowstone National Park by the Yellowstone Center for Resources and the National Park Service is gratefully acknowledged. Discussions with A. Salyers and C. Woese added significantly to the manuscript.

REFERENCES

1) **Barnes, W.M. 1992.** The fidelity of Taq polymerase catalyzing PCR is improved by an N-terminal deletion. *Gene*, **112,** 29-35.

2) **Bargar, K. E.** 1978. Geology and thermal history of Mammoth Hot Springs, Yellowstone National Park, Wyoming.**1444**, 54 p.

3) **Brock, T. D. 1978.** Thermophylic Microorganisms and Life at High Temperatures. Springer-Verlag, New York. 465 p.

4) **Brock, T. D., M. T. Madigan, J. M. Martinko, and J. Parker.** 1999. Biology of Microorganisms, Ninth ed. Prentice Hall. 991 p.

5) **Chao, A. and S-M. Lee.** 1994. Estimating population size via sample coverage for closed capture-recapture models, *Biometrics* **50**, 88.

6) **Colwell, R. K., and J.A. Coddington.** 1994. Estimating terrestrial biodiversity through extrapolation. *Philosophical Transactions of the Royal Society (Series B)* **345**, 101.

7) **Farmer, J. D., and D. J. Des Marais.** 1994. Biological versus inorganic processes in stromatolite morphogenesis: Observations from mineralizing sedimentary systems, p. 61-68. *In* L. J. Stal and P. Caumette (ed.), Microbial Mats: Structure, Development, and Environmental Significance, vol. G35. Springer-Verlag, Berlin Heidelberg. G35: 61-68.

8) **Farmer, J.D.** 2000. Hydrothermal systems: doorways to early biosphere evolution. *GSA Today*, **10**, 1-8.

9) **Fouke, B.W.** 2001. Depositional facies and aqueous-solid geochemistry of travertine-depositing hot springs (Angel Terrace, Mammoth Hot Springs, Yellowstone National Park, USA). Journal of Sedimentary Research, **71**. 497-500.

10) **Fouke, B.W. J.D. Farmer, D.J. Des Marais, L. Pratt, N.C. Sturchio, P.C. Burns, M.K. Discipulo.** 2000. Depositional facies and aqueous-solid geochemistry of travertine-depositing hot springs (Angel Terrace, Mammoth Hot Springs, Yellowstone National Park, USA). *J. Sed. Res*., **70**, 265-285.

11) **Fouke, B.W., G.T. Bonheyo, B.L. Sanzenbacher, J. Frias-Lopez.** 2003. Partitioning of bacterial communities between travertine depositional facies at Mammoth Hot Springs, Yellowstone National Park, U.S.A. *Can. J. Earth Sci.*, 40, 1531-1548 p.

12) **Friedman, I.** 1970. Some investigations of the deposition of travertine from hot springs: I. The isotope chemistry of a travertine-depositing spring. *Geochim. Cosmochim. Acta*, **34**, 1303-1315.

13) **Gressly, A.** 1838. Observations geologiques sur le Jura Solerois. Nouv. Mem. Soc. Helv. Sci. Natur. 2:1-349.

14) **Hugenholtz, P., C. Pitulle, K.L. Hershberger, and N.R. Pace.** 1998. Novel division level diversity in a Yellowstone hot spring. Journal of Bacteriology, **180**. 366-376.

15) **Hughes, J.B., J.J. Hellmann, T.H. Ricketts, B.J.M. Bohannan.** 2001. Counting the uncountable: statistical approaches to estimating microbial diversity. *Applied and Environmental Microbiology* **67**, 4399-4406.

16) **Krebs, C.** 1989. *Ecological methodology* (Harper and Row, New York).

17) **Miller, S.R., and R.W. Castenholz.** 2000. Evolution of thermotolerance in hot spring cyanobacteria of the genus Synechococcus. *Appl. Environ. Microbiol*. **66**, 4222-4229.

18) **Reading, H. G.** 1996. Sedimentary Environments, 3rd ed. Blackwell Science. 688 p.

19) **Sambrook, J., E.F., Fritsch, and T. Maniatis.** 1989. Molecular Cloning. A Laboratory Manual, Cold Spring Harbor Laboratory Press.

20) **Sorey, M.L.,** 1991, Effects of potential geothermal development in the Corwin Springs known geothermal resources area, Montana, on the thermal features of Yellowstone National Park: United States Geological Survey, Water-Resources Investigations Report 91-4052, 110 p.

21) **Sorey, M.L., and E.M., Colvard.** 1997, Hydrologic investigations in the Mammoth Corridor, Yellowstone National Park and vicinity, U.S.A.: Geothermics, v. 26, p. 221-249.

22) **Stackebrandt, E., and B. Goebel.** 1994. Taxonomic Note: a place for DNA-DNA reassociation and 16S rRNA sequence analysis in the present species definition in bacteriology. *Int. J. Syst. Bacteriol*. **44**, 846-849.

23) **Studier, W.F. and J.J. Dunn.** 1983. Complete nucleotide sequence of bacteriophage T7 DNA and the location of T7 genetic elements. Journal of Molecular Biology, **166**. 477-535.

24) **Stumm, W., and J. J. Morgan.** 1981. Aquatic Chemistry. John Wiley and Sons, Ltd., 780 p.

25) **Tindall, K.R., and T.A. Kunkel.** 1988. Fidelity of DNA synthesis by the *Thermus aquaticus* DNA polymerase: *Biochemistry*, **27**, 6008-6013.

26) **Tucker, M. E., and V. P. Wright.** 1996. Carbonate Sedimentology. Blackwell Science, Oxford. 482 p.

27) **Vieira, J., and J. Messing.** 1982. The pUC plasmids, an M13mp7-derived system for insertion mutagenesis and sequencing with synthetic universal primers. Gene (Amsterdam), **19**. 259-268.

28) **Walker, R. G., and N. P. James.** 1992. Facies Models: Response to Sea Level Change, vol. 1. Geological Association of Canada.

29) **Wilmotte, A., G. Van der Auwera, and R. DeWachter.** 1993. Structure of the 16S ribosomal RNA of the thermophilic cyanobacterium Chlorogloeopsis HTF

(Mastigocladus laminosus HTF) strain PCC7518, and phylogenetic analysis. FEBS Letters, **317**. 96-100.

30) **Wilson, J. L.** 1975. Carbonate Facies in Geologic History. Springer-Verlag, New York. 472 p.

Fig 1. Location of Spring AT-1 at Angel Terrace in the Mammoth Hot Springs complex of Yellowstone National Park. Shading depicts the surface area covered by the Spring AT-1 waters as the water flows away from the vent (shown by a ●).

Fig. 2. Field photograph of Spring AT-1 at Angel Terrace in the Mammoth Hot Springs complex of Yellowstone National Park. Note the large well-developed terraced travertine pool in the center of the photograph.

Fig. 3. Schematic cross-section view of Spring AT-1 of indicating travertine depositional facies distributions, sample locations, travertine mineralogy, spring water temperature and pH, and spring water flow directions, and rates of travertine precipitation.

Fig. 4. Species present in all Spring AT-1 travertine facies using the 1% OTU definition. Each OTU is numbered sequentially, starting with OTUs that first appear in the vent facies, followed by OTUs that first appear in the apron and channel, then the pond, then the proximal-slope facies, and lastly the distal-slope facies. The figure provides a graphical representation of where each OTU (*y*-axis) is found (*x*-axis).

Fig. 5. Accumulation curve generated for all Spring AT-1 travertine facies using the 1% OTU definition.

Fig. 6. Accumulation curves generated for the Spring AT-1 pond facies using the 3%, 1%, and 0.5% OTU definitions. Accumulation curves for different OTU definitions collapse into the same curve when the *x* and *y*-axis are properly scaled by the total number of OTUs and samples.

1

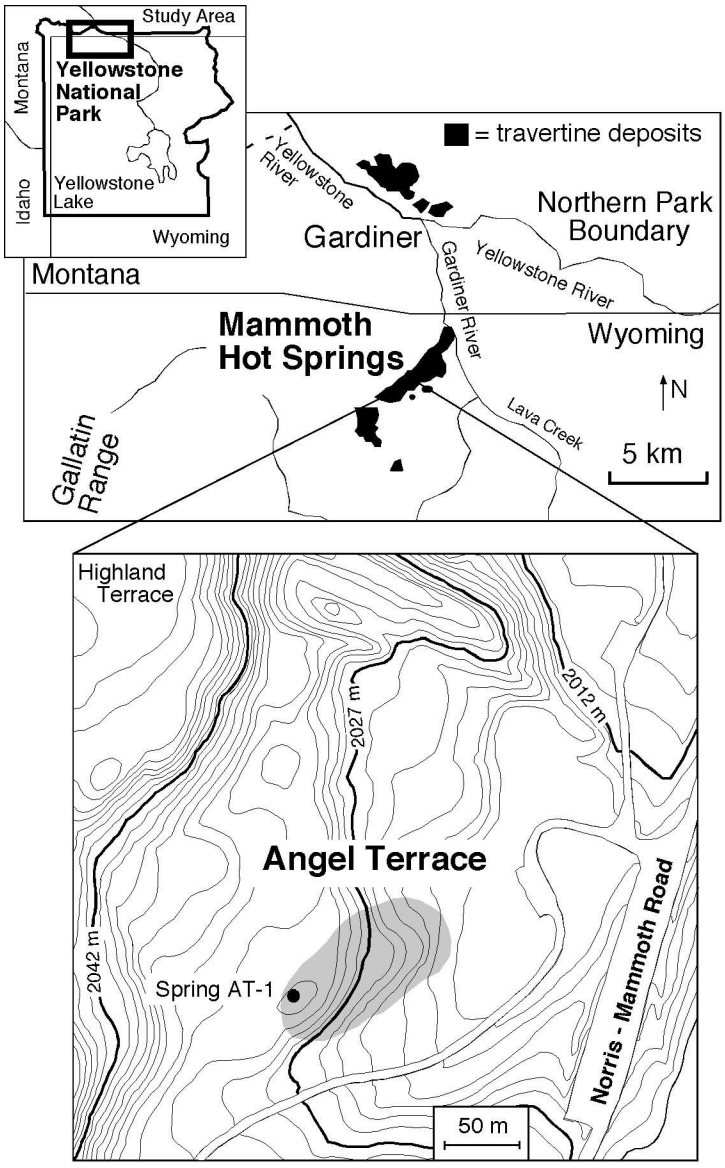
Study Area
Montana
Yellowstone National Park
Yellowstone Lake
Idaho
Wyoming
= travertine deposits
Yellowstone River
Gardiner
Northern Park Boundary
Gardiner River
Yellowstone River
Montana
Wyoming
Mammoth Hot Springs
N
Lava Creek
5 km
Gallatin Range
Highland Terrace
2027 m
2012 m
Angel Terrace
2042 m
Spring AT-1
Norris - Mammoth Road
50 m

2

3 Figure 1


Vent Facies
Apron and Channel Facies
Pond Facies
Proximal Slope Facies
1 m

Figure 2

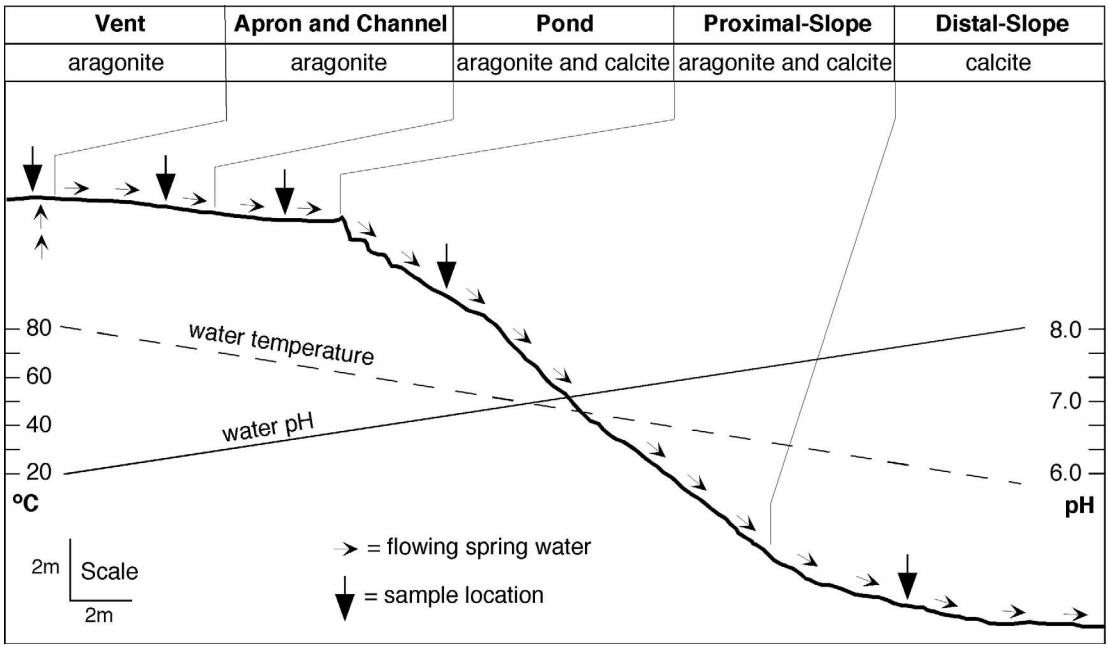
Vent
Apron and Channel
Pond
Proximal-Slope
Distal-Slope
aragonite
aragonite
aragonite and calcite
aragonite and calcite
calcite
80
60
40
20
°C
water temperature
water pH
8.0
7.0
6.0
pH
2m
Scale
2m
= flowing spring water
= sample location

Figure 3

1

2

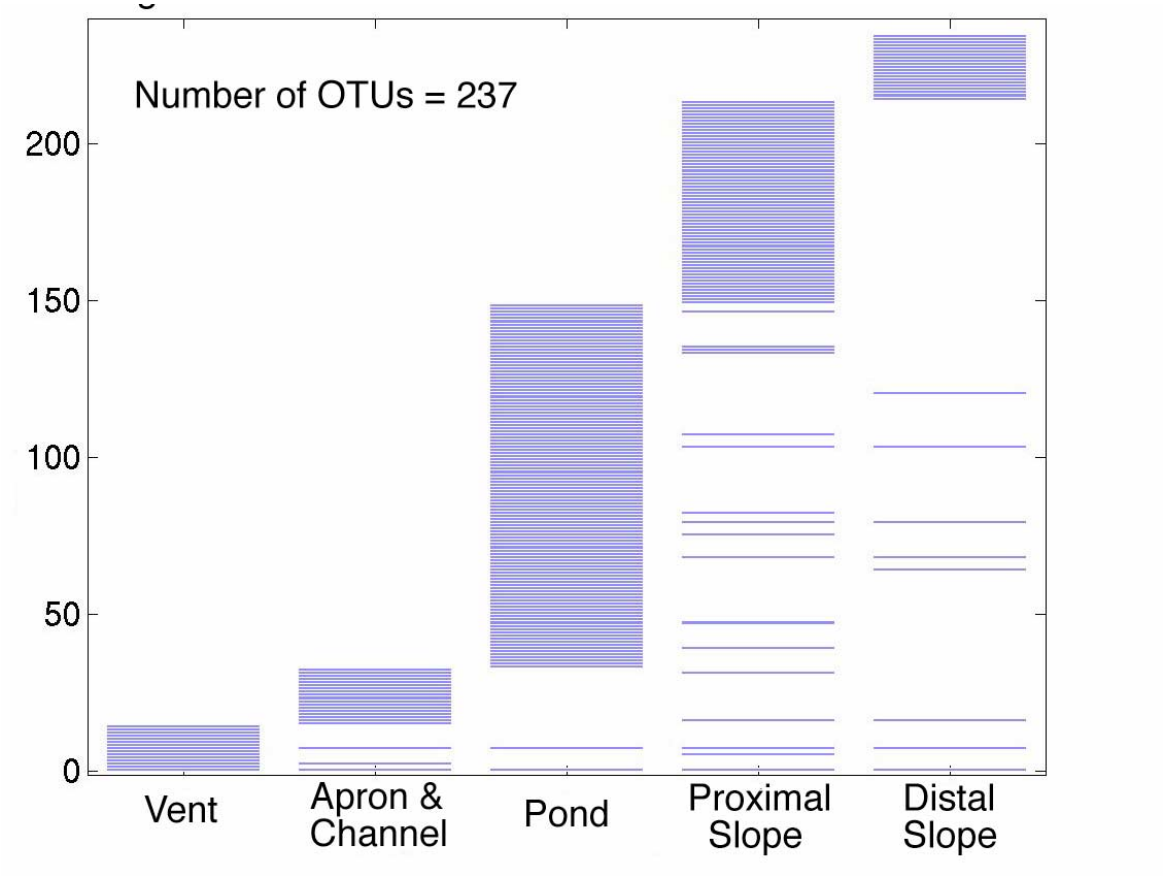

3

4

5 Figure 4.

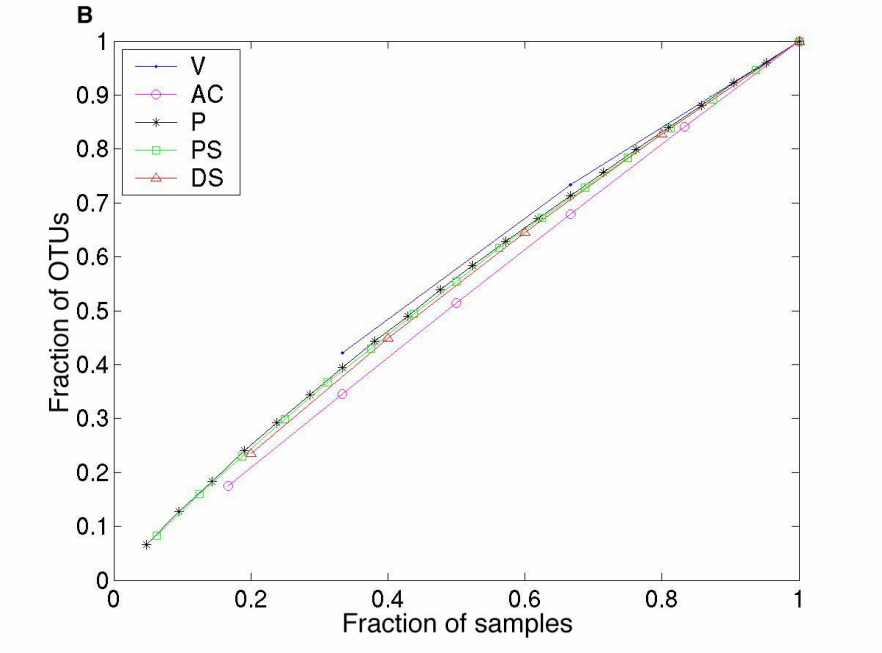
B
V
AC
P
PS
DS
Fraction of OTUs
Fraction of samples
0
0.1
0.2
0.3
0.4
0.5
0.6
0.7
0.8
0.9
1
0.2
0.4
0.6
0.8

Figure 5

1

2

3

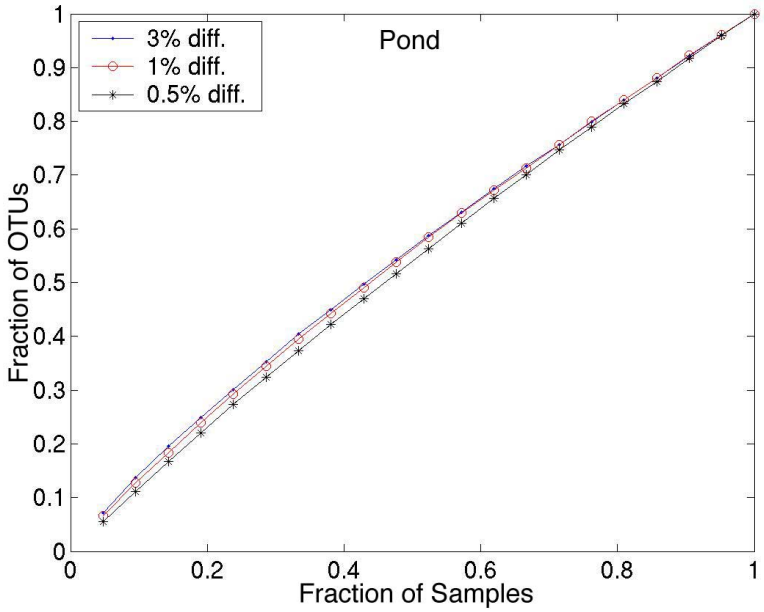

4

5 Figure 6

6